

## RESEARCH ARTICLE

# Synthesis, Characterization and Cytotoxic Evaluation of Graphene Oxide Nanosheets: *In Vitro* Liver Cancer Model

Samah A Loutfy<sup>1</sup>, Taher A Salaheldin<sup>2,3\*</sup>, Marwa A Ramadan<sup>4</sup>, Khaled Yehia Farroh<sup>3</sup>, Zeinab F Abdallah<sup>1</sup>, Tareq Youssef<sup>4</sup>

### Abstract

**Background:** Graphene nanosheets have a broad spectrum of biomedical applications. Hepatocellular cancer (HCC) is a major health problem in the Egyptian population. Currently, treatment strategies are invasive and have several adverse side effects. Thus, other approaches are required for managing this aggressive type of cancer. Our objective here was to prepare and characterize graphene oxide nanosheets and evaluate cytotoxic effect at the molecular level in an *in vitro* human liver cancer cell model (HepG2). **Methods:** Graphene oxide nanosheets were generated by chemical oxidation and characterized by transmission electron microscopy and X-ray diffraction. Cytotoxic effects in HepG2 cells were monitored by sulforhodamine B (SRB) colorimetric assay followed by flow cytometric analysis. Molecular investigations of DNA fragmentation and expression of some apoptotic genes at the transcriptional RNA level were also performed. **Results:** Treatment of HepG2 cells with 400 µg/ml graphene oxide nanosheets showed alteration in cell morphology after 24 h. Flow cytometry revealed accumulation of cells in S phase of cell cycle followed by dramatic effects on cellular DNA. Extensive evaluation of the cytotoxic effects of graphene oxide showed increased mRNA Bax apoptotic gene expression with not of P53 and caspase-3 mRNA after 24h, suggesting involvement of an intrinsic apoptotic caspase-independent pathway. **Conclusion.** Graphene oxide can mediate apoptotic gene signaling in human liver cancer cells opening a novel approach to cancer management. Further analyses at the molecular level are now required to confirm our results and facilitate biomedical applications *in vivo*.

**Keywords:** Graphene oxide nanosheets- HepG2 cells- cytotoxic effects- PCR

*Asian Pac J Cancer Prev*, **18** (4), 955-961

### Introduction

Graphene, a novel carbon-based nanomaterial, has attracted a great deal of attention due to its extraordinary physical, chemical, and biological characteristics. Graphene has sparked enormous interest in many research groups around the world. Graphene nanosheets, a one-atom-thick planar sheet of carbon atoms densely packed in a honeycomb crystal lattice demonstrates distinct structural properties allowing its functional modifications, rendering it an attractive candidate for broad range of biomedical applications include: biosensor development, imaging, drug delivery, bacterial inhibition, and photothermal therapy. (Liu et al., 2010; Wang Y et al., 2009; Peng et al., 2010) In recent years, graphene oxide nanosheets (GO), a heavily oxygenated graphene derivative having high stability in aqueous dispersion, has been extremely explored for biomedical applications such as *in vitro* drug delivery and cellular imaging. (Peng et al., 2010; Liu et al., 2008; Sun et al., 2008) GO has also

been employed as a drug carrier for controlled loading and release of antitumor agents. (Zhang et al., 2009) Further, GO has been projected as a novel biosensing platform for detection of various biomolecules. In addition, it can lead to photothermal ablation of tumors following intravenous administration in animals this because of its strong optical absorption in the near-infrared range. This renders it a promising tool in the field of biomedical applications (Jung et al., 2010 ; He et al., 2010).

Hepatocellular carcinoma (HCC) is one of the most common type of cancer among Egyptian population where most patients suffered from poor prognosis and tumor recurrence. However, there are many strategies for treating HCC but all of them are very expensive, time consuming, and have several side effects in addition poor efficiency due to multidrug resistance. Therefore another approaches are still required for managing such aggressive type of cancer. Recently, many nanoparticles have been used as anti-cancer therapy employed in solving the complex problems of multidrug resistance

<sup>1</sup>Virology and Immunology Unit, Cancer Biology Department, National Cancer Institute, <sup>4</sup>Department of Photochemistry Photobiology, National Institute for Laser Enhanced Science (NILES), Cairo University, <sup>2</sup>Mostafa Elsayed Center for Nanotechnology Research, British University in Egypt, <sup>3</sup>Nanotechnology and Advanced Materials Central Lab, Agricultural Research Center, Egypt. \*For Correspondence: Taher.salah@bue.edu.eg

(Swami et al., 2012) or even playing an increasing role in the development of novel diagnostic methods. The currently approved nanoparticle systems have in some cases improved the therapeutic index of drugs by reducing drug toxicity or enhancing drug efficacy. However, many studies have shown that nanomaterials may have positive effect on cancer treatment, some of them still are not well understood such that recently developed Graphene or Graphene oxide (Kennedy et al., 2014).

The current study aims to evaluate the cytotoxic effects of GO on human liver cancer cells (HepG2 cells) at a cellular and molecular level in order to understand nature of cell death and apoptotic pathway accompanied with Graphene oxide.

## Materials and Methods

### *Synthesis of graphene oxide (GO)*

GO were prepared using modified Hummers method (Hummers and Offeman, 1958; Park S and Ruoff R, 2009). 0.5g of graphite (99.9995%, Alfa Aesar, WardnHill, MA, USA) was dissolved in 25ml of sulfuric acid (95%, H<sub>2</sub>SO<sub>4</sub>, Sigma-Aldrich, St. Louis, MO, USA), and 0.5g of sodium nitrate (99.9%, NaNO<sub>3</sub>, Sigma-Aldrich, St. Louis, MO, USA) was added to the solution under stirring for 15min. the reaction vessel was transferred to Ice bath and the temperature was adjusted below 10oC, potassium permanganate (99.9%, KMnO<sub>4</sub>, Sigma-Aldrich, St. Louis, MO, USA), was slowly added, 3g over 10min. To get homogenous GO, the temperature must not elevated over 10oC during the addition of KMNO<sub>4</sub>. The reaction mixture was stirred at 35oC overnight. 50ml of deionized water was slowly added, the temperature of the reaction elevated and must adjusted around 90oC under stirred for 1h. Finally, 140ml of warm deionized water was added and then 5ml of hydrogen peroxide (H<sub>2</sub>O<sub>2</sub>, 36%, Alfa Aesar, WardnHill, MA, USA). Brownish yellow graphene Oxide were formed. Dry GO were obtained by three washing cycles using water and centrifugation at 5000rpm for 30min then dried at 60oC. Exfoliation of GO was approached by sonication (200w) of GO in deionized water for 1h generating well dispersed GO.

### *Characterization of GO*

The synthesized GO was processed for physicochemical. Spectra absorption were recorded using a double beam UV-Vis spectrophotometer (Cary 5000, Agilent, USA). The morphology of GO was imaged using High Resolution Transmission electron Microscope (HRTEM, Tecnai, G20, FEI, Netherlands), operating at an accelerating voltage of 200kV. A drop from a dilute GO solution was deposited on carbon coated-copper grid and left to evaporate at room temperature forming a monolayer. Zeta potential was measured by zeta sizer (Nano ZS, zeta sizer, Malvern, UK) based on the dynamic light scattering technique. X-ray Diffraction (XRD) technique was used for phase analysis. XRD patterns were recorded in the scanning mode on XDR instrument (X'pert PRO, PAN analytical, Netherlands) operated at 40kV and a current of 30mA with Cu K radiation (= 1.54Å) and High score plus software. The diffraction intensities were compared

with the standard International Centre for Diffraction Data (ICDD) library. Powder Diffraction File (PDF-4) database gave the information about the crystal structure of the GO. The preparation and characterization of GO was conducted at the Nanotechnology and Advanced Materials Central Laboratory, Agriculture Research Center, Egypt.

### *Cell culture*

Human liver hepatocellular carcinoma (HepG2) cell line was cultured and maintained in RPMI 1640 media (Biowest, France) supplemented with 10% fetal bovine serum (Biowest, France), antibiotics (100IU/ml 2% penicillin-streptomycin) and 0.5% fungizone (Biowest, France). The cells were maintained in monolayer culture at 37°C under a humidified atmosphere of 5% CO<sub>2</sub>. The cells were sub-cultured by trypsinization (0.025% trypsin in 0.0025% EDTA, Biowest, France) and maintained in tissue culture laboratory at the National Cancer Institute, Cairo University, with cryogenic banking of low-passage cells to maintain uniformity of cell properties through the study. Cell numbers and viability were monitored by standard Trypan blue dye exclusion procedures and growth curves for HepG2 was determined under baseline conditions prior to investigation of cytotoxicity (Loutfy, Shalaby, et al., 2015).

### *Cytotoxicity assay*

Serial dilutions of graphene oxide were prepared in 2% RPMI 1640 media giving concentrations of 125, 250, 500 and 1000µg/ml. Cytotoxicity was evaluated using Sulforhodamine B (SRB) assay. Positive and negative controls were run in each plate. Negative controls (cells with media only; untreated cells), were set as 100% viability. Cells subjected to osmotic shock (treated with distilled water) were taken as positive controls (zero viability) were used to subtract background from all optical density (OD) values. Morphological changes of cells were followed by phase contrast microscopy (40x magnifications). The percent of viability was estimated based on the following equation:

$$\% \text{Viability} = (\text{Mean OD of test sample}) / (\text{Mean OD of negative control}) \times 100$$

### *Cellular uptake of GO*

HepG2 cells were treated with the 400µg/ml graphene oxide for 24h. Cells were washed with PBS buffer then fixed with 2% glutaraldehyde for 2 hours and washed twice with PBS before fixation in 1% Osmium tetroxide for 1 hour. Following agarose (1.5%) enrobing, Spurr's resin embedding, and ultrathin (50nm) sectioning, the samples were stained with 2% aqueous uranyl acetate and 25mg/ml lead citrate and imaged with Transmission Electron Microscope (HRTEM, Tecnai, G20, FEI, Netherlands) (Zhu Z J et al., 2008).

### *Flow cytometric cell cycle analysis*

Cellular effect of GO on different phases of HepG2 cell cycle was analyzed using a MoFlo flow cytometer (Dako Cytomation, Glostrup) (Nunez R, 2001). HepG2 cells (5x10<sup>5</sup> cells/well) were plated in 6-well microplates.

After treatment with the double concentration of obtained GO IC<sub>50</sub> for 24h, cells were washed twice with PBS, suspended in 300µl of PBS (pH 7.3), and finally fixed with 4ml of ice-cold 70% ethanol. To stain with propidium iodide (PI), Cells sedimentation was performed by centrifugation, the ethanol was removed and cells washed once with PBS. The cell pellets were then resuspended in 1ml of PI/Triton X-100 staining solution (0.1% Triton X-100 in PBS, 0.2 mg/ml RNase A, and 10mg/ml PI) and incubated for 30 minutes at room temperature.

#### DNA fragmentation

Fragmentation of cellular DNA was investigated following treatment of HepG2 cells with the double concentration of IC<sub>50</sub> for 24h. A fixed amount (100ng) of extracted cellular DNA (Genomic DNA Purification Kit, Amersham Biosciences) was subjected to 1.5% agarose gel electrophoresis in Tris-acetate buffer pH (8.2), stained with 0.5µg/ml ethidium bromide. The bands were examined under UV trans-illumination and photographed. Smearing, or presence of many low molecular weight DNA fragments, is a characteristic feature of apoptotic cells (Loutfy, Al-Ansary, et al., 2015; Loutfy, Shalaby, et al., 2015).

#### Detection of cellular apoptotic genes expression by One-Step reverse transcriptase polymerase chain reaction

Extensive evaluation of the cytotoxic effect of Go on the expression of apoptotic genes (P53, Bax, and caspase-3) at the transcriptional level using one-step reverse-transcription polymerase chain reaction (RT-PCR) assay was performed after treatment of HepG2 with GO at concentration of double IC<sub>50</sub> for 24h. The β-actin housekeeping gene was detected in each run to ensure RNA integrity. The detection of mRNA was previously optimized at different annealing temperatures. (Loutfy et al., 2016)

## Results

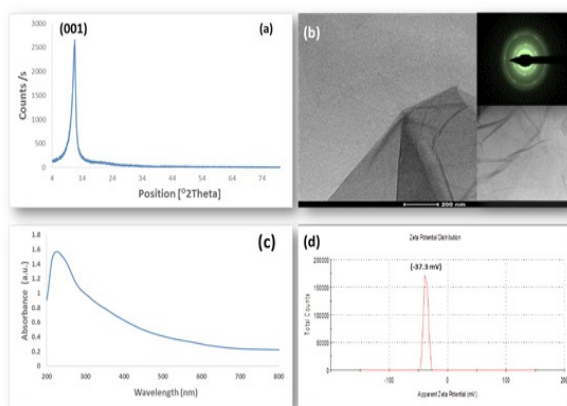


Figure 1. Characterization of GO. a: X-Ray Diffraction Pattern. b: High Resolution Transmission Electron Microscope image and Selected Area Electron Diffraction pattern. c: UV-vis-NIR plasmonic absorption band. d: Zeta potential measured by Dynamic Light Scattering.

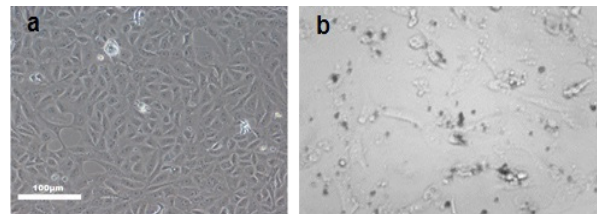


Figure 2. a) Control HepG2 cell Line b) HepG2 Cells incubated with 400µg/ml Graphene Oxide for 24 h, Light Microscopy (Phase Contrast, 40x)

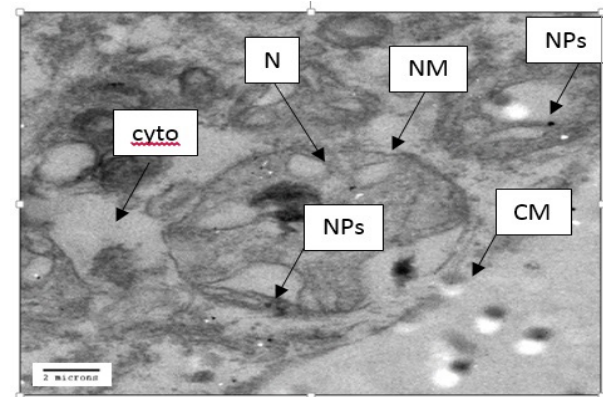


Figure 3. Localization of GO in HepG2 Cells by Transmission Electron Microscope Indicated: Nps, (Nanoparticles); CM, (Cell Membrane); Cyto, (Cytoplasm); N, (Nucleus); NM, (Nuclear Membrane) At Magnification Of 8,000 Times.

#### Synthesis and Characterization of Graphene oxide

GO was prepared by oxidation of graphite using modified Hummers method, a combination of potassium permanganate and sulfuric acid producing diamanganese heptoxide (Mn<sub>2</sub>O<sub>7</sub>) active oxidant that oxidizes the unsaturated double bonds of graphite forming graphene oxide (Dreyer et al., 2010). Figure 1a showed XRD pattern which displayed a narrow and sharp peak at  $2\theta = 10.86^\circ$  which corresponds to the (001) reflection plane of GO with inter-planar d-spacing about 0.81nm that is much larger than that of graphite (0.34nm). The increased d-spacing of GO due to the presence of abundant oxygen-containing functional groups on both sides of the graphene caused by the oxidation (Yan-Li et al., 2011). High Resolution Electron Transmission Microscopic imaging (HR-TEM), Figure 1b showed ultrathin sheet-like structure, smooth

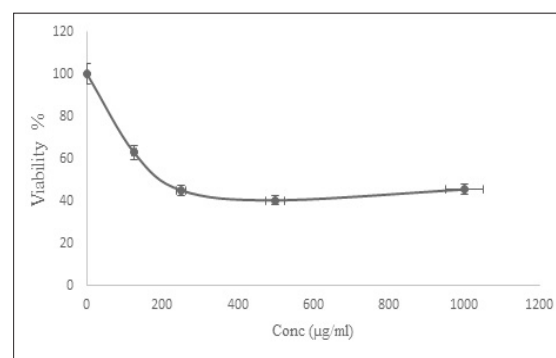


Figure 4. Cytotoxicity Assay at Different Concentrations (µg/ml) of Graphene Oxide on HepG2 Cells

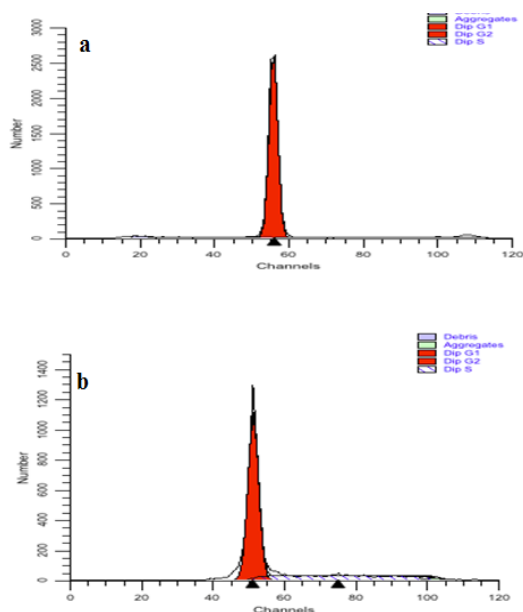


Figure 5. Cell Cycle Analysis of GO on HepG2 A) untreated HepG2 Cells B) HepG2 Cells treated with 400µg/ml graphene oxide

surface, and wrinkled edge GO nanosheet. The Selected Area Electron Diffraction (SAED) pattern showed single layer of GO nanosheet is approximately 6µm in size and 4nm thick and indicate the crystalline structure of GO. Spectrophotometric measurement of graphene oxide solution showed no absorption at the visible region but showed intense characteristic absorption peak at ~230,

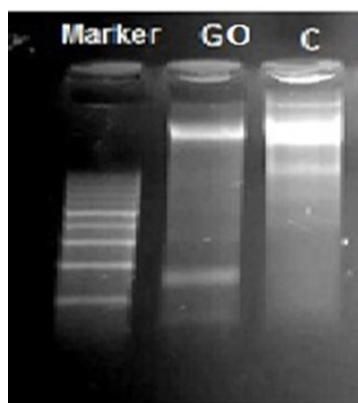


Figure 6. EB-Stained Gel Electrophoresis of Genomic DNA Extraction from Untreated and Treated HepG2 Cell Line. Lane 1 is 100bp ladder, Lane 2 (treated cells with 400µg/ml of GO) and lane 3 (untreated cells)

Table 1. Flow Cytometry Analysis for Graphene Oxide on HepG-2

|  | % G1 Phase | % G2 Phase | % S phase | % Diploid |
|--|------------|------------|-----------|-----------|
| HepG2 cells (untreated)                  | 93.9       | 0.24       | 5.84      | 100       |
| HepG-2 cells treated with Graphene oxide | 75.0       | 0.00       | 25.00     | 100       |

Table 2. Genomic DNA Content in DNA Fragmentation Assay after Treatment with Graphene Oxide

| Sample  | Conc. ng/ul | Ratio 260/280 |
|---|-------------|---------------|
| untreated HepG2 cells                             | 377         | 1.95          |
| HepG-2 cells treated with 400µg/ml Graphene oxide | 34.8        | 1.85          |

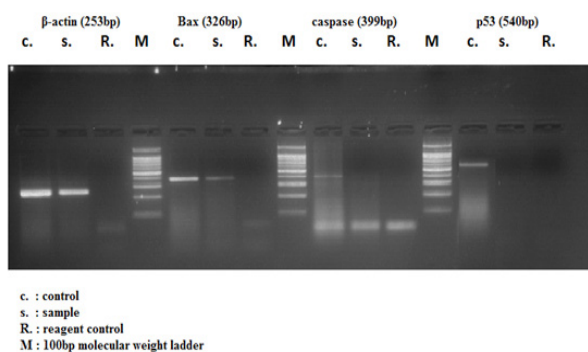


Figure 7. EB-Stained Gel Electrophoresis of Genomic Mrna Expression From Untreated (c.) and treated HepG2 (s.), Lane 1, untreated HepG2; Lane 2, HepG2 treated with 400µgGO; Lane 3, Reagent control; Lane 4, Ladder (100bp); Lane 5, untreated cells; Lane 6, HepG2 treated with 400µgGO; Lane 7, Reagent control; Lane 8, ladder; Lane 9, untreated cells; Lane 10, treated cells with 400µg GO100; Lane 11, Reagent; lane 12, Ladder; Lane 13, HepG2 untreated; Lane 14, treated cells with 400µgGO; lane 15, Reagent control; Lanes 1-3, β actin mRNA expression at 253bp, Lanes 5-7: Bax mRNA gene at 326 bp, Lanes 9-11: Caspase-3 mRNA at 399 bp, Lanes 13-15: P53 mRNA at 540 bp

Figure 1c. The surface charge of GO was represented by zeta potential measurement using Dynamic Light Scattering (DLS) technique, that was found to be high negative (-37.3mV), Figure 1d.

Interaction of GO with HepG2 cells

Light microscopy

HepG2 cells were treated with 400µg/ml of GO for 24h showed morphological alteration compared to untreated cells as shown in Figure 2.

Transmission electron microscopy

Transmission electron microscopy (TEM) images demonstrated binding and internalization of Graphene oxide into HepG2 cells. Aggregation of GO to form clusters on the cell membrane is evident Figure 3. Examination of images at higher magnification showed intracellular clusters, mainly associated with membranes, the most dispersed particles were in cytoplasm. Moreover, treatment with GO showed to be associated with disruption and fragmentation of intracellular organelles with its localization into nucleus, nuclear membrane and mitochondria.

### Cytotoxic effect of GO on HepG2 cells

The cytotoxic effect of various concentrations of GO was assessed in HepG2 cell cultures using SRB colorimetric assay after 48h time interval. Results showed that IC50 was 213µg/ml Figure 4.

### Effect of GO on cell cycle analysis

Our prepared GO was further investigated by flow cytometric analysis of cell cycle and DNA contents of cells after treatment with 400µg/ml for 24h. Untreated cells showed the expected cell cycle pattern for continuously growing cells, whereas treated cells showed decrease in cell number in G1 phase and marked accumulation of cells in S phase 25% compared to only 5% in case of the untreated one, Table 1 and Figure 5.

### DNA fragmentation of GO

DNA fragmentation analysis was carried out to investigate the genotoxic effects of GO on cellular DNA. DNA fragmentation characteristic of late apoptosis was observed after treatment with GO at concentration of 400µg/ml for 24h where it dramatically affected concentration of DNA (34ng/ul) compared to untreated cells (377ng/ul), Table 2 and Figure 6.

### Apoptotic genes expression as detected by One-Step RT PCR

Our results showed that β-actin housekeeping gene was nicely expressed in both treated and untreated cells indicating integrity of genomic RNA expression. All studied apoptotic genes (mRNA of P53, Bax and caspase-3) were expressed in untreated HepG2 but only mRNA Bax gene was expressed in cells treated with GO at concentration of 400µg/ml for 24h Figure 7.

## Discussion

Graphene oxide nanosheets were synthesized by chemical oxidation of graphite according to the most commonly used methods, Hummer's method and its modified versions (Niyogi et al., 2006; Shahriary and Athawale, 2014). Surfaces and edges of individual sheets of GO decorated with oxygen functional groups (Lerf et al., 1998) and due to ionization of carboxyl groups, which are primarily present at the edges of sheet, enable GO to be electrostatically stabilized form a colloidal suspension in water, alcohols, and certain organic solvents without need for surfactants (Paredes et al., 2008). TEM image, figure 1b showed well-formed 4nm extended sheet of multi-layer GO where exfoliation of graphene oxide into individual sheets can be facilitated by ultrasonic agitation or rapid heating (McAllister et al., 2007) but excessive ultra-sonication can result in the decrease of lateral dimensions (Sun et al., 2008). It is important to note that the reaction mixture contains oxidation of graphite results in a brown-colored viscous slurry, which include graphene oxide and exfoliated sheets along with non-oxidized graphitic particles and residue of the oxidizing agents. After repeated centrifugation, sedimentation, or dialysis, salts and ions from the oxidation process can be removed from nearly pure GO suspensions (Li et

al., 2008). XRD pattern, figure 1a, illustrated that GO was formed in a highly purified and crystalline form. Narrow and high intense characteristic peak at  $2\theta = 10.86^\circ$  which corresponds to the (001) reflection plan of GO with inter-planer d-spacing about 0.81nm that is much larger than that of graphite (0.34nm). The increased d-spacing of GO due to the presence of abundant oxygen-containing functional groups on both sides of the graphene caused by the oxidation (Yan-Li et al., 2011). Graphene oxide has no absorption bands in the visible region, figure 1c, but showed broad maximum absorption band in the ultraviolet region at ~230 nm attributable to  $\pi-\pi^*$  transition of the atomic C-C bonds (Xu, Yong, and Wu, 2013). The surface of GO sheets is mostly negatively charges due to presence of free carboxylic groups on edges that was clearly observed from zeta potential measurements by DLS, Figure 1d. The average surface potential was -37.3mV enable it to form stable solution in water and facilitate its absorption by cellular membrane.

Previous studies have demonstrated biomedical applications of Graphene oxide especially as antitumor activities. (Loh et al., 2010) In the current study HepG2 in vitro model of human liver cancer cells was used because this disease is considered one of the commonest cancer diseases among Egyptian population, and newer approaches is still required to replace the traditional one which has several disadvantages.

Previously Lammel and coworkers have studied the cytotoxic effect of GO on HepG 2 cells using 4 different cell viability assays. They concluded that GO caused a dose dependent decrease in the cell viability. This was in agreement with our results which showed that treatment of HepG2 with our engineered GO at concentration of 125ug/ml decreased cell viability to 40% and at concentration of 1,000ug/ml decreased the cell viability to 60% after 48h of cell exposure. This effect as explained before was due to strong physical interactions of GO with phospholipid layer, resulting in loss of plasma membrane integrity and its damage. This was also obviously demonstrated by alteration of cell morphology compared to the untreated cells. In addition, this was evidenced by TEM images which showed penetration of GO through plasma membrane and its internalization into cytoplasm, mitochondria and nucleus. It has been reported that GO penetrate cells by piercing and mechanically disrupt plasma membrane and aggregated inside cells.(Lammel et al., 2013)

Jaworski and coworkers have reported that graphene platelets at a concentration of 100µg/ml reduced the viability of human glioblastoma U87 and U118 cells to 54% and 60% respectively. (Jaworski et al., 2013) Moreover, Chang and team work have observed that GO induce oxidative stress in adenocarcinoma human alveolar basal epithelial cells (A549) at concentration of 10mg/ml.(Chang et al., 2011) All these observations indicate that several factors control cytotoxic effect of GO and hence its application in cancer therapy, include these parameters: chemistry, size, surface charge, shape, concentration and type of cell line.

Therefore, our engineered GO was subjected to further biological investigations on a cellular and molecular level.

Regarding flow cytometric analysis, results showed that treatment of HepG2 with 400ug/ml of GO for 24h caused cell accumulation in S phase indicating cell damage, this was confirmed by its genotoxic effect on cellular DNA as evidenced by results of DNA fragmentation assay. Mechanism of the apoptotic effect induced by GO was further analyzed by expression of some apoptotic genes like P53, Bax and caspase-3 on the RNA level after cell treatment with 400ug/ml GO for 24h. Results showed that no expression of P53 mRNA in treated cells this can be explained by i) expression level of P53 was too low to be detected by our PCR assay especially it is one version PCR assay, ii) P53 has short half-life and may be degraded, therefore it should be monitored at different time intervals and on a protein level before reaching to a solid conclusion. Also, our results showed no expression of caspase-3 mRNA suggesting that apoptotic effect of GO was exerted via a caspase independent pathway but such results need further investigations. It has been reported that ROS production can mediate poly ADP-ribose polymerase-1 (PARP-1) activation, and PARP-1 activation is necessary for AIF (apoptotic inducing factor) release from mitochondria. AIF has been found to be the major important caspase-independent proapoptotic factor which is released from mitochondria and translocate into nucleus to cleave DNA and ultimately cell death. (Hongmei et al., 2012) Moreover, previous reports have demonstrated ability of GO to induce the generation of intracellular Reactive Oxygen Species (ROS) depending on dose and time of exposure and they referred variations in results of previous studies to GO size, preparation protocol and type of cell line. (Liao et al., 2011; Chang et al., 2011) In agreement with our results, it has been reported that Bax and Bax like proteins might mediate caspase-independent death via piercing mitochondrial outer membrane. Accordingly, this may further support caspase independent apoptotic pathway for our engineered GO till we perform further investigations on different concentrations and at different time interval. Conversely, Li and coworkers have shown that GO activate apoptosis in macrophages through the involvement of caspase-3. (Li et al., 2012) However this effect was observed in different type of cells it is quiet relevant to analyze the protein expression of these apoptotic genes.

Graphene oxide showed cytotoxic effect at concentration of 400ug/ml on HepG2 after 24h of cell exposure as demonstrated by flow cytometry and cellular fragmentation. Flow cytometry results revealed cell cycle arrest at S phase and dramatic effect on cellular DNA. This was further confirmed by no expression of P53 and caspase mRNA with expression of genomic Bax mRNA. Graphene oxide can mediate the apoptotic gene signaling of human liver cancer cell opening a new approach in cancer management. Further analysis is still required to evaluate impact of graphene oxide on expression level of apoptotic proteins.

## Reference

- Chang YL, Yang ST, Liu JH, et al (2011). In vitro toxicity evaluation of graphene oxide on A549 cells. *Toxicol Lett*, **200**, 201-10.
- Dreyer DR, Park S, Bielawski CW, et al (2010). The chemistry of graphene oxide. *Chem Soc Rev*, **39**, 228-40.
- He QY, Sudibya HG, Yin ZY, et al (2010). Centimeter-long and large-scale micropatterns of reduced graphene oxide films: Fabrication and sensing applications. *ACS Nano*, **4**, 3201-8.
- Hongmei Z, Ji Yean K, Hisashi N, et al (2012). Apoptosis and medicine. Eds Tobias M. Ntuli. InTech, Croatia.
- Hummers WS, Offeman RE (1958). Preparation of graphitic oxide. *J Am Chem*, **80**, 1339.
- Jaworski S, Sawosz E, Grodzik M, et al (2013). In vitro evaluation of the effects of graphene platelets on glioblastoma multiforme cells. *Int J Nanomed*, **8**, 413-20.
- Jung JH, Cheon DS, Liu F, et al (2010). Graphene oxide based immuno-biosensor for pathogen detection. *Angew Chem Int Ed*, **49**, 5708-11.
- Kennedy DC, Gil GO, Lai CH, et al (2014). Carbohydrate functionalization of silver nanoparticles modulates cytotoxicity and cellular uptake. *J Nanobiotechnology*, **12**, 59-66.
- Lammel T, Boisseaux P, Fernandez-Cruz ML, Navas JM (2013). Internalization and cytotoxicity of graphene oxide and carboxyl graphene nanoplatelets in the human hepatocellular carcinoma cell line HepG2. *Part Fibre Toxicol*, **10**, 253-8.
- Lerf A, He H, Forster M, Klinowski J (1998). Structure of graphite oxide revisited. *J Phys Chem B*, **102**, 4477-82.
- Li D, Marc BM, Scott G, et al (2008). Processable aqueous dispersions of graphene nanosheets. *Nat Nanotechnol*, **3**, 101-5.
- Li Y, Ying L, Yujian Fu, et al (2012). The triggering of apoptosis in macrophages by pristine graphene through the MAPK and TGF signaling pathways. *Biomaterials*, **33**, 402-11.
- Liao K-H, Yu-Shen L, Christopher W, et al (2011). Cytotoxicity of graphene oxide and graphene in human erythrocytes and skin fibroblasts. *ACS Appl Mater Interfaces*, **3**, 2607-15.
- Liu Y, Yu D, Zeng C, et al (2010). Biocompatible graphene oxide-based glucose biosensors. *Langmuir*, **26**, 6158-60.
- Liu Z, Robinson JT, Sun X, Dai H (2008). PEGylated Nano-graphene oxide for delivery of water insoluble cancer drugs. *J Am Chem Soc*, **130**, 10876-7.
- Loh KP, Qiaoliang B, Goki E, Manish C (2010). Graphene oxide as a chemically tunable platform for optical applications. *Nat Chem*, **2**, 1015-24.
- Loutfy SA, Hanaa MAE, Mostafa HE, et al (2016). Synthesis, characterization and cytotoxic evaluation of chitosan nanoparticles: in vitro liver cancer model. *Int J Nanomedicine*, **7**, 1-9.
- Loutfy SA, Nadia AA, Nour TA, et al (2015). Anti-proliferative activities of metallic nanoparticles in an in vitro breast cancer model. *Asian Pac J Cancer Prev*, **16**, 6039-46.
- Loutfy SA, Rokaya H, Shalaby AR, et al (2015). Evaluation of cytotoxic effect of metallic nanoparticles in an in vitro liver cancer model. *J Chem Pharm Res*, **7**, 470-87.
- Mc A, Michael J, Je-Luen L, et al (2007). Single sheet functionalized graphene by oxidation and thermal expansion of graphite. *Chem Mater*, **19**, 4396-404.
- Niyogi S, Bekyarova E, Itkis ME, et al (2006). Solution properties of graphite and graphene. *J Am Chem Soc*, **128**, 7720-1.
- Nunez R (2001). DNA measurement and cell cycle analysis by flow cytometry. *Curr Issues Mol Biol*, **3**, 67-70.
- Paredes JI, Villar-Rodil S, Martínez-Alonso A, Tascón JMD (2008). Graphene oxide dispersions in organic solvents. *Langmuir*, **24**, 10560-4.
- Park S, Ruoff R (2009). Chemical methods for the production of graphenes. *Nat Nanotechnol*, **4**, 17-24.
- Peng C, Hu W, Zhou Y, et al (2010). Intracellular imaging with

- a graphene-based fluorescent probe. *Small*, **6**, 1686–92.
- Shahriary, L, Anjalía A (2014). Graphene oxide synthesized by using modified hummers approach. *Int J Renew Energy Environ Eng*, **2**, 58-63.
- Sun X, Liu Z, Welsher K, et al (2008 ). Nano-graphene oxide for cellular imaging and drug delivery. *Nano Res*, **1**, 203–12.
- Swami A, Jinjun S, Suresh G, et al (2012). Multifunctional nanoparticles for drug delivery applications. Eds Svenson, Sonke, Prud'homme and Robert K. Springer US, Boston, MA, pp 9–29.
- Wang Y, Li YM, Tang LH, et al (2009). Application of graphene-modified electrode for selective detection of dopamine. *Electrochem Commun*, **11**, 889–92.
- Xu S, Liu Y, Peiyi W (2013). One-pot, green, rapid synthesis of flower-like gold nanoparticles / reduced graphene oxide composite with regenerated silk fibroin as efficient oxygen reduction electrocatalysts. *ACS Appl Mater Interfaces*, **5**, 654-62.
- Yan-Li C, Hu Z, Chang Y, et al (2011). Zinc oxide/reduced graphene oxide composites and electrochemical capacitance enhanced by homogeneous incorporation of reduced graphene oxide sheets in zinc oxide matrix. *J Phys Chem*, **115**, 2563–71.
- Zhang L, Xia J, Zhao Q, et al (2009). Functional graphene oxide as a nanocarrier for controlled loading and targeted delivery of mixed anticancer drugs. *Small*, **6**, 537–44.
- Zhu ZJ, Ghosh PS, Miranda OR, et al (2008). Multiplexed screening of cellular uptake of gold nanoparticles using laser desorption/ionization mass spectrometry. *J Am Chem*, **130**, 14139–43.